CHEMISTRY OF MATERIALS

Article

pubs.acs.org/cm

Carbonophosphates: A New Family of Cathode Materials for Li-Ion Batteries Identified Computationally

Hailong Chen,[†] Geoffroy Hautier,[†] Anubhav Jain,[†] Charles Moore,[†] Byoungwoo Kang,[†] Robert Doe,[†] Lijun Wu,[‡] Yimei Zhu,[‡] Yuanzhi Tang,[§] and Gerbrand Ceder*[,†]

[†]Department of Materials Science and Engineering, Massachusetts Institute of Technology, 77 Massachusetts Ave, Cambridge, Massachusetts 02139, United States

[‡]Brookhaven National Laboratory, Upton, New York 11973, United States

[§]School of Engineering and Applied Sciences, Harvard University, Cambridge, Massachusetts 02138, United States

Supporting Information

ABSTRACT: The tremendous growth of Li-ion batteries into a wide variety of applications is setting new requirements in terms of cost, energy density, safety, and power density. One route toward meeting these objectives consists in finding alternative chemistries to current cathode materials. In this Article, we describe a new class of materials discovered through a novel high-throughput ab initio computational approach and which can intercalate lithium reversibly. We report on the synthesis, characterization, and electrochemical testing of this novel lithium-carbonophosphate chemistry. This work demonstrates how the novel high-throughput computing approach can identify promising chemistries for next-generation cathode materials.

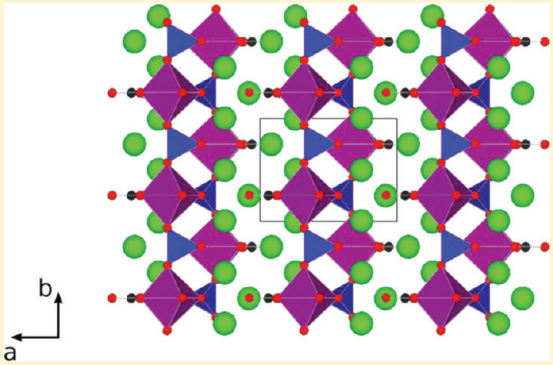

KEYWORDS: *carbonophosphate, lithium battery, cathode, hydrothermal, ion-exchange, ab initio, high-throughput*

INTRODUCTION

Since their commercial introduction in the early 1990s, lithium-ion batteries now power applications from portable electronics to electric vehicles. A critical element of a Li-ion battery is the Li-intercalation cathode material as it determines much of the energy and power density of the battery. There are currently only a handful of cathode materials that can meet the commercial requirements in terms of energy density, safety, rate capability, and cost.[1,2]

Chemists and material scientists traditionally search for new materials by a subtle combination of chemical intuition and serendipity.[3] In a departure to those traditional materials design approaches, we have set up a high-throughput ab initio computational environment[4] capable of screening thousands of potential new materials. Such ab initio calculations have already helped researchers understand[5−9] known materials and guided their optimization.[10,11] In this computational route to materials discovery, new chemistries are suggested by compound prediction algorithms[12,13] that data-mine known information in the Inorganic Crystal Structure Database (ICSD).[14] These candidates are then rapidly evaluated for their voltage, stability, and lithium diffusivity[15] using high-throughput computing, thereby providing reliable and unbiased guidance toward promising new chemistries.

Following this computational approach we have identified recently the lithium−carbonophosphates as a new class of potential cathode materials.[16] This class of compounds has the potential to retain the safety of $LiFePO_4$ while having a theoretical specific energy that is almost 50% greater. In this work, we present follow-up computations and present the synthesis and electrochemical test results of two representative compounds of this chemical family identified computationally: the iron and manganese lithium carbonophosphate.

COMPUTATIONAL AND EXPERIMENTAL METHODS

All ab initio computations were performed using the plane-wave based Vienna ab initio Simulation package (VASP)[17] within the projector augmented-wave approach[18] using the generalized gradient exchange and correlation functional parametrized by Perdew−Burke−Ernzerhof.[19] We used a U parameter[20] for the transition metals (for Fe, U = 4 eV; Mn, U = 3.9 eV; Co, U = 5.7 eV; Ni, U = 6 eV). An energy cutoff of 520 eV was used for all computations.

A k-point density of at least 500/(number of atoms in unit cell) k-points was used for all the Brillouin integrations. The Monkhorst−Pack method was used to obtain k-points distributed as uniformly as possible.[21] A Γ-centered grid was used for hexagonal cells.

Accurate structural parameters (lattice parameters and atomic positions) were obtained with a higher convergence criteria than that was used for the energy optimization (5×10^{-7} eV for electronic convergence and 5×10^{-5} eV for ionic convergence).

Received: October 28, 2011
Revised: May 3, 2012
Published: May 31, 2012

All computations were performed with spin polarization. All magnetic moments were initialized in a ferromagnetic configuration with high spin initialization for the transition metals. More details on the high-throughput ab initio methodology can be found in Jain et al.[4] The activation barriers for diffusion were evaluated using nudge elastic band computations in GGA-PAW-PBE without any U parameter.[22,23]

$Na_3FeCO_3PO_4$ and $Na_3MnCO_3PO_4$ were synthesized using a hydrothermal method. In a representative synthesis of $Na_3MnCO_3PO_4$, 0.02 mol $MnNO_3{\cdot}4H_2O$ was dissolved in 50 mL of water to form a clear solution A. 0.02 mol of $(NH_4)_2HPO_4$ and 20 g of Na_2CO_3 were dissolved in 100 mL of water to form a clear solution B. Solution A was then quickly added to solution B under fast magnetic agitation. The mixture slurry was then transferred to a sealed glass bottle and heated at 120 °C for 70 h with magnetic stirring in an Ar flushed glovebox. After the bottle was slowly cooled down to room temperature, the products were washed several times first with distilled water and then with methanol, followed by drying in a vacuum oven at 40 °C overnight. The procedure for $Na_3FeCO_3PO_4$ synthesis is identical, except that $FeSO_4{\cdot}7H_2O$ was used as the transition metal source and the mixing of the solutions was done in an Ar flushed glovebox to prevent possible oxidation of Fe(II) to Fe(III).

The Li version of these carbonophosphates were obtained through a Li−Na ion exchange method,[24] using about 500 mg of as-synthesized Na compounds as starting materials and 2 M LiBr in 1-hexanol as the solution. The ion exchange of $Na_3MnCO_3PO_4$ was employed for 4 days at 130 °C. The ion exchange of $Na_3FeCO_3PO_4$ was done at 110 °C for 3 days. The ion exchange products were separated from the solution by centrifuging and washed first with methanol, and then with distilled water and methanol again to remove the salts.

All the powder samples were characterized by X-ray diffractions using a Rigaku RU3000 (Copper Kα, λ = 1.5406 Å) or a Rigaku miniflex II diffractometer (Chromium Kα, λ = 2.2897 Å). Some of the samples were characterized by using synchrotron radiation at beamline X16C and X14A at the National Synchrotron Light Source at Brookhaven National Laboratory (NSLS-BNL). The scanning electron microscope (SEM) images were taken using a JEOL 6032 SEM. The transmission electron microscope (TEM) images and selected area electron diffraction (SAED) patterns were obtained with a JEM 2100F HRTEM operated at 200 KV. Refinement and whole pattern fitting of the X-ray diffraction (XRD) patterns were performed using the GSAS code.[25]

For electrochemical characterization, the as-prepared sample was mixed with poly vinylidene fluoride (PVDF) binder and carbon (super P) (6: 1: 3 wt %) in *N*-methyl pyrrolidone (NMP) to make a thick slurry. The slurry was deposited on aluminum foil by using a doctor-blade method and dried at 80 °C overnight. Some samples were ball milled with the ratio of active material: carbon = 85%: 15% (wt %) for 1 h at 400 rpm. The ball milled samples were then mixed with binder and super P carbon, where the overall ratio of active material: carbon: binder is 6: 3: 1 (wt %). Coin cells (CR2016) were assembled in an argon-filled glovebox. Each cell typically contained about 2−4 mg of active materials, separated from the Li foil anode by a piece of Celgard separator (Celgard, Inc., U.S.A.). A 1 M solution of $LiPF_6$ in ethylene carbonate/dimethyl carbonate (1:1) was used as the electrolyte. Electrochemical experiments were carried out on a battery cycler (Arbin Instruments, College Station, TX) in galvanostatic mode at various rates.

RESULTS

I. Computational Results. The procedure for the high-throughput computational approach is described in Figure 1. For more than 10,000 compounds, consisting of both known compounds (from the ICSD database)[14] and new compounds proposed by data mining algorithms,[12,13] we computed using density functional theory (DFT) several materials properties: voltage[26] and Li migration barriers[27,28] were calculated with a method published elsewhere. Stability was determined by comparing the compound's energy to all possible linear

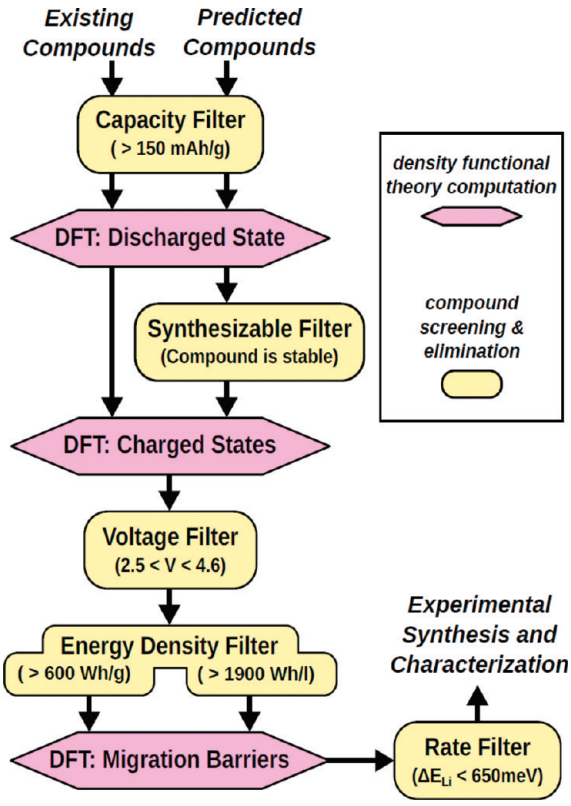

Figure 1. Schematic flowchart showing the general procedure of battery materials search and screening using a DFT based high-throughput computational approach.

combination of compounds in the ICSD database[14] which would give the same composition (convex hull construction). Special attention was given to stable sodium compounds which may have a metastable lithium equivalent, as it is possible to transform these into each other by a lithium−sodium ion-exchange. Li−Na ion-exchange has been successfully used to synthesize novel cathode materials.[24,29,30] Compounds satisfying the stability criteria were further screened on specific gravimetric (>600 Wh/kg) and volumetric (>1900 Wh/l) energy density in the voltage window of stability for current commercial electrolytes (<4.6 V) and on lithium migration barrier.

Our computational approach differs from traditional materials design in two ways. First, the scale of the screening effort (about 10,000 compounds) is much higher than that can be tested in a traditional experimental laboratory. Second, the computations revealed strengths and weaknesses of each compound prior to synthesis, allowing the experimental team to focus their efforts only on the most promising candidates. These characteristics of the computational approach provide the opportunity to significantly accelerate the materials discovery process.

One class of materials identified by this search is the carbonophosphates with a general formula of $A_3M(CO_3)(PO_4)$ (A = Na or Li; M = Co, Mn, Fe, or Ni).[31] While the sodium versions of the Mn and Fe compounds are known as rare minerals, respectively named sidorenkite[32−34] and bonshtedtite,[35] there are no reports of their artificial synthesis, and their Ni and Co versions have never been reported. Moreover, no lithium-containing carbonophosphate has ever been observed; this may help explain why they were thus far unexplored as

dx.doi.org/10.1021/cm203243x | *Chem. Mater.* 2012, 24, 2009−2016

cathodes. Sidorenkite ($Na_3MnCO_3PO_4$) and bonshtedtite ($Na_3FeCO_3PO_4$) are isostructural and crystallize in the monoclinic $P2_1/m$ (11) space group. Figure 2 shows their

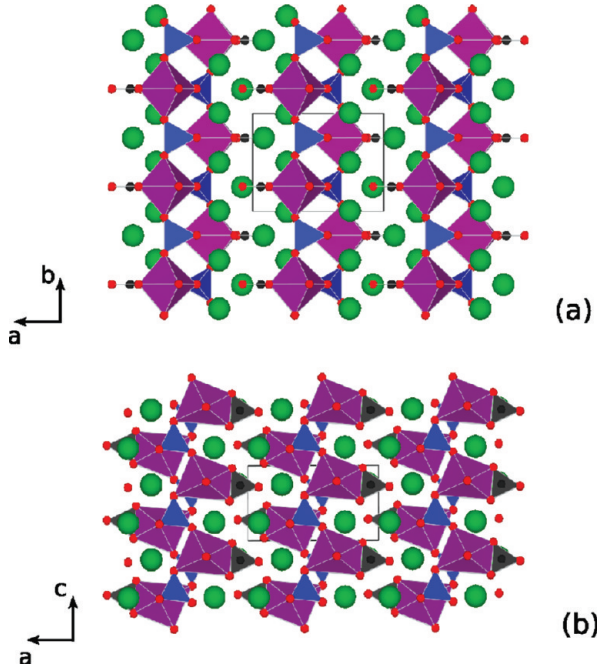

Figure 2. Structure of the $Na_3MPO_4CO_3$ compounds (M = Mn, Fe, Co, Ni, etc.) viewing down from *c* axis (a) and *b* axis (b). Purple: transition metal octahedron; black: CO_3 group; blue: PO_4 group; green: alkaline metal.

crystal structure in a 2 × 2 × 2 super cell. The unit cell is outlined in black. Each transition metal octahedron (purple) shares 4 vertices with tetrahedral PO_4 groups (blue) and an edge with a CO_3 group (black). The two-dimensional subunits extending along the (100) plane are composed of connected transition metal octahedra, PO_4 groups and CO_3 groups. Alkali metals (green) connect those two-dimensional subunits. The alkalis occupy two different sites, coordinated by 7 and 6 oxygen atoms respectively.

Computationally, Na carbonophosphate for M = Co, Mn, Fe, and Ni are all found to be stable at 0 K. Hence, in addition to the Mn and Fe carbonophosphate that have been found in nature, the computations suggest that it should also be possible to synthesize the Co and Ni carbonophosphate. The Li versions, on the other hand, are all predicted to be moderately unstable (see Supporting Information), suggesting the need to synthesize those compounds through Li−Na ion exchange from the Na versions. Computations indicate that Li−Na exchange will cause ~11% volume change, major contraction along the *a* axis (5%), and a deviation from the 90 degrees lattice angles (see Supporting Information).

The computed Li-extraction voltages (vs lithium metal) for the $Li_3M(CO_3)(PO_4)$ compounds are shown in Figure S1 (Supporting Information). The Fe- (Fe^{2+}/Fe^{3+}: 3 V), Mn- (Mn^{2+}/Mn^{3+}: 3.2 V and Mn^{3+}/Mn^{4+}: 4.1 V), and Co- (Co^{2+}/Co^{3+}: 4.1 V) based compounds are predicted to be electrochemically active in this structure in the voltage range suitable for current electrolytes. Volume changes upon delithiation are predicted to be low: 1.1% for Fe (after one lithium removed) and 2.4% for Mn (after 2 lithium removed). The Mn carbonophosphate is a possible two-electron system, with a computed theoretical energy content of 859 W h/kg and 2376 W h/l. This is a 45% and 15% improvement in terms of gravimetric and volumetric energy density compared to the most successful polyanion-based cathode material currently used, namely, $LiFePO_4$.[36] It would also represent a significant gravimetric energy density improvement over $LiMnPO_4$ (664 W h/kg), which is currently under intense investigations as a potential successor to $LiFePO_4$.[37]

Finally, the last step of our screening involves a computational screening on lithium mobility. We investigated the lithium mobility in $Li_xMn(PO_4)(CO_3)$ by evaluating lithium ion vacancy migration barriers ab initio with the nudged elastic band framework.[28,38,39] Activation barriers for net lithium vacancy migration (see Supporting Information) were calculated to be 396 meV for $Li_3MnCO_3PO_4$, 478 meV for $Li_2MnCO_3PO_4$ and 380 meV for $LiMnCO_3PO_4$. These values are qualitatively similar to those calculated for α-$Li_{1.5}TiO_2$,[38] and I−Li_2NiO_2[39] and indicate that lithium diffusivity should not limit the activity of the manganese carbonophosphate[39]

II. Experimental Results. On the basis of the computational results, both $Li_3FeCO_3PO_4$ and $Li_3MnCO_3PO_4$ were synthesized through Li−Na ion-exchange from the stable sodium phases. As we previously mentioned, no laboratory synthesis of $Na_3FeCO_3PO_4$ and $Na_3MnCO_3PO_4$ have been reported. The natural sidorenkite mineral decomposes around 600 °C and releases CO_2,[32] implying that it is not possible to synthesize this compound through conventional solid state reaction at temperatures above 600 °C. Solid state reaction at lower temperature might be an alternative, but because of the much lower reactivity of the starting materials and reaction kinetics, the reaction may take too long or not take place at all. Alternatively, hydrothermal synthesis is a viable approach given the formation conditions for carbonophosphates in the earth's crust.[32]

Phase-pure $Na_3FeCO_3PO_4$ and $Na_3MnCO_3PO_4$ were successfully obtained by hydrothermal synthesis after optimization of the heating temperature, time, and the concentration of starting materials in the solutions. Figure 3a shows the XRD pattern and Rietveld refinements of the synthetic $Na_3FeCO_3PO_4$ using the structure model proposed by Khomyakoy et al.[35] Lattice parameters extracted from the refinement are listed in Table 1 (wRp = 0.0772, χ^2 = 3.205). The composition of the synthetic material, tested by inductive coupled plasma-atomic emission spectrometry (ICP), shows an elemental ratio of Na: Fe: *P* = 2.93: 1.11: 0.96, fairly close to stoichiometry (3:1:1). The synthetic $Na_3FeCO_3PO_4$ is a light green precipitate, but its color changes to very light brown after washing with distilled water, which may indicate oxidation of Fe(II) on the surface because of the short exposure to air and/or the air in distilled water during washing. To avoid significant oxidation of Fe(II), the hydrothermal reaction and the following washing process were performed in an Ar-flushed glovebox, and the powder was dried overnight in a vacuum oven at 40 °C.

Figure 3b and Table 1 show the XRD and refinement results for the synthetic $Na_3MnCO_3PO_4$ sample (wRp = 0.0598, χ^2 = 4.87) using the structure model proposed by Kurova et al.[33,34] The elemental ratio in $Na_3MnCO_3PO_4$, as tested by ICP, is Na: Mn: *P* = 3.01: 1: 0.98. The color of the powder is light beige. The Mn compound appears stable when exposed to air, and the synthesis and washing can be performed outside the glovebox. In this study, we kept all processes in the Ar glovebox for consistent comparison with the Fe compound.

dx.doi.org/10.1021/cm203243x | *Chem. Mater.* 2012, 24, 2009−2016

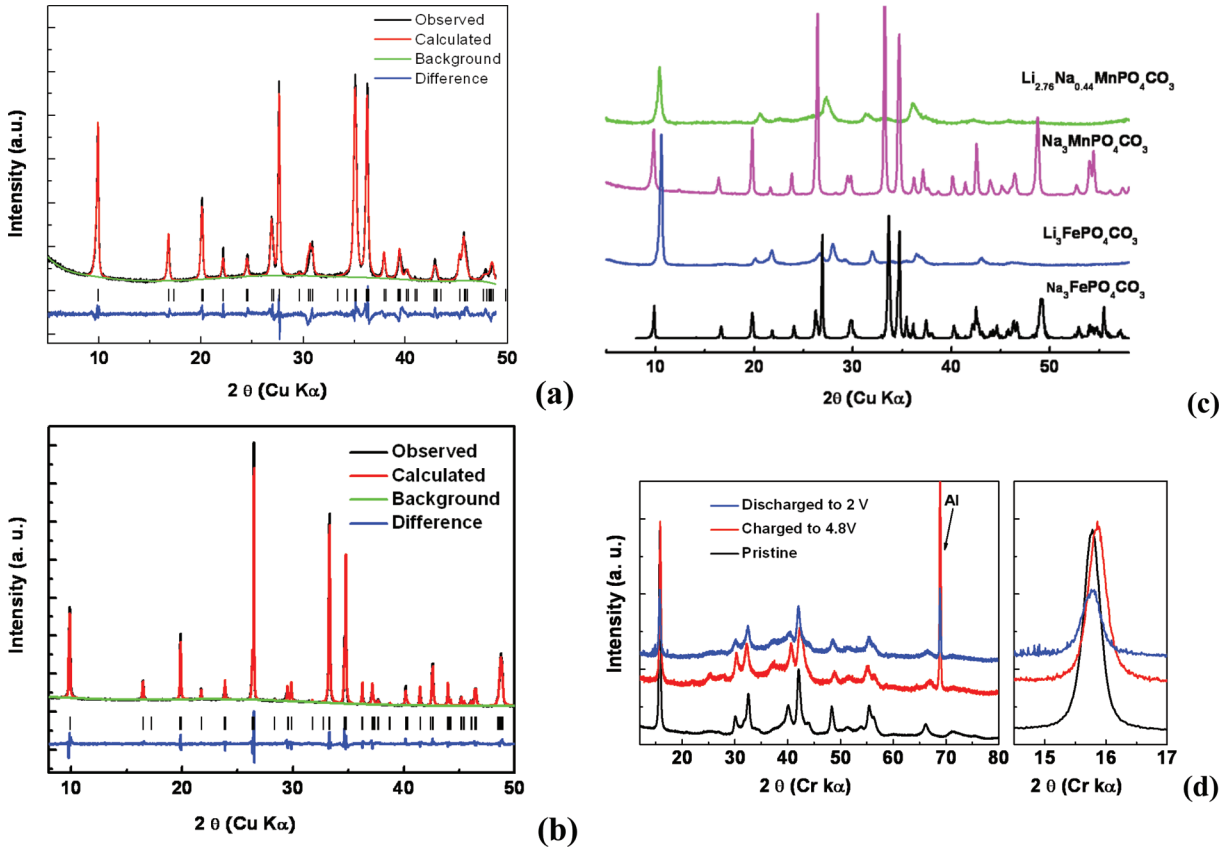

Figure 3. X-ray diffraction data of the carbonophosphates. (a) and (b): The high resolution synchrotron XRD patterns and corresponding refinements of synthetic bonshteditite (a) and sidorenkite (b) (converted to Cu Kα wavelength). (c) XRD patterns of Fe and Mn compounds before and after Li–Na ion-exchange. (d) XRD patterns of pristine $Li_3FePO_4CO_3$ powder (black) and $Li_3FePO_4CO_3$ cathode film charged to 4.8 V (red) and film charged to 4.8 V then discharged to 2 V (blue) charging. The reflections from Al foil current collector are also labeled.

Table 1. Cell Parameters of the Synthetic Samples and Natural Minerals[26–29]

compound	a (Å)	b (Å)	c (Å)	α (deg)	β (deg)	γ (deg)	V (Å^3)
$Na_3FePO_4CO_3$ (synthetic)	8.929	6.602	5.159	90.000	89.662	90.000	304.189
$Na_3FePO_4CO_3$ (mineral)	8.921	6.631	5.151	90.000	90.250	90.000	304.71
$Na_3MnPO_4CO_3$ (synthetic)	8.988	6.739	5.162	90.000	90.131	90.000	312.78
$Na_3MnPO_4CO_3$ (mineral)	8.997	6.741	5.163	90.000	90.16	90.000	311.16
$Li_3FePO_4CO_3$ (pristine sample)	8.44	6.402	4.93	88.1	94.8	94.5	264.7
$Li_2FePO_4CO_3$ (charged sample)	8.36	6.290	4.99	86.43	93.83	91.71	261.1

In scanning electron microscopy (SEM), both the Fe and Mn compounds synthesized by hydrothermal reaction at 120 °C for 70 h show a plate-like morphology, with the aspect ratio being not particularly large (Figure 4a and 4b, respectively). The particle size (~500 nm) is quite uniform for both samples.

Li–Na ion exchange was performed using 2 M LiBr in 1-hexanol solution[24] in an Ar-flushed glovebox, with the Fe compound heated for 3 d at 110 °C and the Mn compound for 4 d at 130 °C. The samples were washed with methanol and distilled water to remove extra salts after ion-exchange. As shown in Figure 4c and 4d, ion exchange does not change the particle size of either sample, but the edges and surfaces become less sharp. However, some structural changes did occur upon ion exchange as are apparent in Figure 3c, which shows the XRD patterns of both Fe and Mn samples before and after ion-exchange. Despite significant changes to the pattern, the characteristic major peak of the sidorenkite structure, located at 10° 2θ and corresponding to the {100} planes, is still present after ion-exchange. The XRD line shape of the ion-exchanged samples is much broader than that for the Na precursors. Since the particle size did not change significantly, the peak broadening is likely due to smaller domain size or the presence of defects, such as stacking faults (see TEM characterization in Supporting Information, Figure S4). The stacking faults could be caused either by exfoliation from the organic solvents or by local ordering of residual Na and Li ions.

By combining single crystal electron diffraction under transmission electron microscopy (TEM) and synchrotron X-ray powder diffraction, we observed that the structure of $Li_3FeCO_3PO_4$ transforms from monoclinic to triclinic after ion-exchange. From the ab initio computations, we find that the lowest energy structure of the Li compound is approximately the same as its Na precursor, with the polyhedra slightly turned and tilted so that the 2-fold axis and mirror plan present in the $P2_1/m$ space group are lost and only the inversion symmetry is preserved, giving the computed cell $P\bar{1}$ symmetry (see Supporting Information). Although the poorly crystallized nature of the ion-exchanged sample prevents accurate atomic

dx.doi.org/10.1021/cm203243x | *Chem. Mater.* 2012, 24, 2009–2016

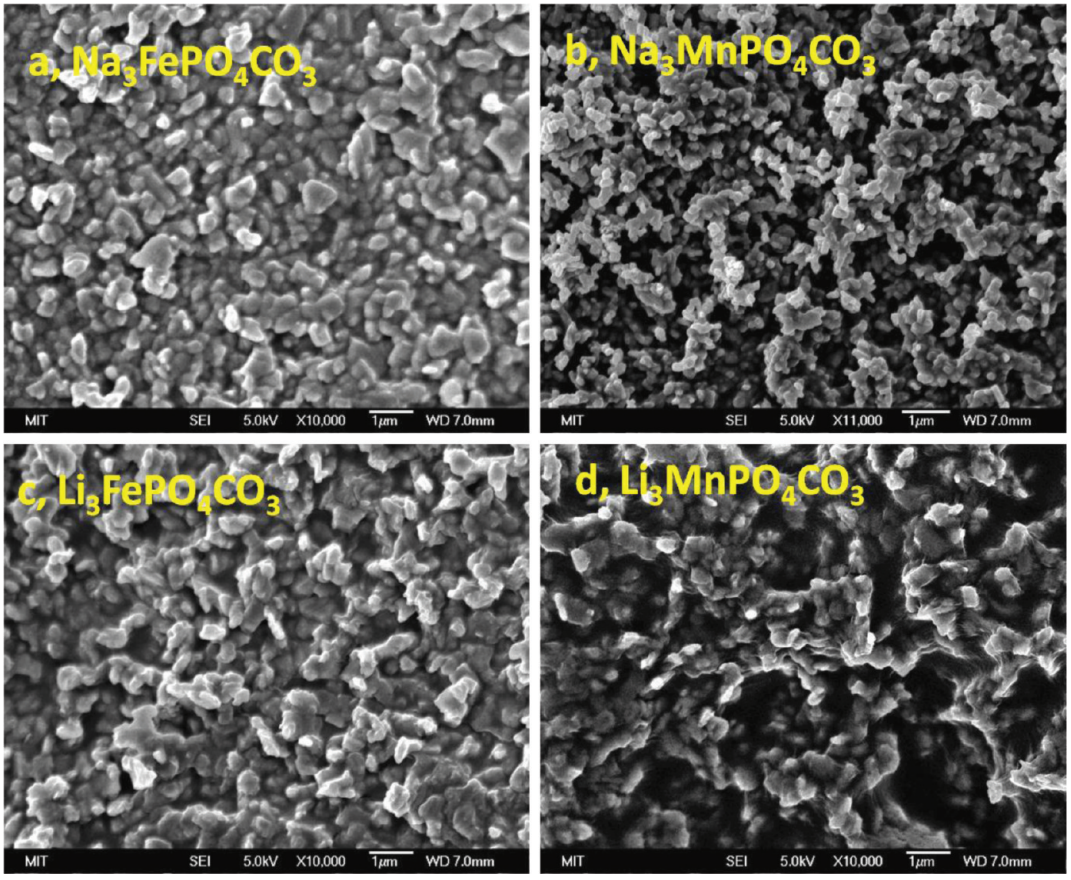

Figure 4. SEM image of Fe and Mn samples before and after ion-exchange: (a) $Na_3FePO_4CO_3$; (b) $Na_3MnPO_4CO_3$; (c) $Li_3FePO_4CO_3$, and (d) $Li_3FePO_4CO_3$. The scale bars are 1 μm.

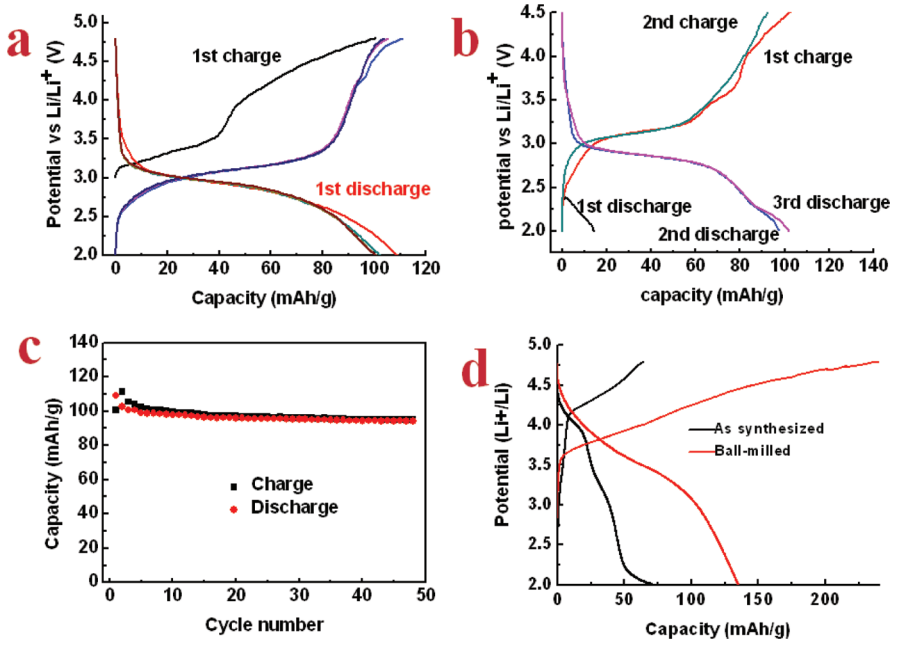

Figure 5. (a) Voltage profile of ball-milled stoichiometric $Li_3FePO_4CO_3$ cycled at C/5 rate at 2−4.5 V at room temperature. (b) The voltage profile of nonball-milled stoichiometric $Li_3FePO_4CO_3$ cycled at 2−4.5 V at 60 °C and C/10 rate, starting with discharge first. (c) The capacity retention of condition (a). (d) The voltage profile of $Li_{2.67}Na_{0.63}Mn_{0.96}PO_4CO_3$, both ball-milled and nonball-milled samples, cycled at C/100 rate at room temperature. No voltage holding or resting was applied at the end of charge and discharge for all the cells.

positions to be obtained by Rietveld refinement, the cell parameters of the sample can be obtained from single particle electron diffraction (see Supporting Information, Figure S5) and whole pattern fitting of the XRD patterns (see Supporting

dx.doi.org/10.1021/cm203243x | *Chem. Mater.* 2012, 24, 2009−2016

Information, Figure S6a). The resulting cell parameters are listed in Table 1. The volume of the unit cell shrinks ~12% for the Fe compound after ion exchange, in agreement with our DFT calculation.

Atomic composition analysis using ICP was also performed on all samples after ion-exchange. The results show that the ion-exchange is almost 100% complete for the Fe sample, with the element ratio being Li: Na: Fe: P = 2.95: 0.08: 1.01: 0.95. However, ion-exchange for the Mn samples appears to be more difficult. Even after being ion-exchanged for 4 days at 130 °C, only a portion of the Na is replaced by Li, with the element ratios being Li: Na: Mn: P = 2.67: 0.63: 0.96: 1. Longer exchange time (up to one month), higher temperature (up to 150 °C) or repeatedly exchanging did not significantly increase the ratio of Li: Na in the final product. This may indicate that a fairly stable phase exists close to this composition that prevents further Na exchange.

The ion-exchanged $Li_3FeCO_3PO_4$ and $Li_{3-x}Na_xMnCO_3PO_4$ samples were ball-milled with 15 wt % carbon black and electrochemically tested in coin cells. The Fe (Mn) sample was ball-milled at 400 (600) rpm for one (6) hour(s). For comparison, samples without ball milling were also tested under the same conditions. In both cases, the electrode compositions were kept the same, for example, the ratio of active material: total carbon: binder was set as 6: 3: 1. In these preliminary tests, high carbon content in the cathode film was used to minimize any rate limiting factors from the electrode design. For the ball-milled $Li_3FeCO_3PO_4$ sample, the first discharge capacity is 110 mAh/g at C/5 rate, matching the theoretical capacity of 115 mAh/g. In subsequent cycles a stable capacity of ~100 mAh/g is obtained between 2 and 4.5 V (see Figure 5a and c). When $Li_3FeCO_3PO_4$ was tested without ball milling, only ~40 mAh/g was obtained at C/10, indicating a transport limitation in the electrode or active material. At 60 °C, almost full theoretical capacity could be cycled even without ball milling as shown in Figure 5b. These results imply that the capacity of this material at room temperature might be limited by kinetic factors when at 500 nm particle size. The plateau at 3.0 V in the voltage curve is consistent with the computed voltage for the Fe^{2+}/Fe^{3+} redox couple in this structure.

From the XRD patterns of pristine, charged, and discharged $Li_3FePO_4CO_3$ samples in Figure 4d, it is clear that the unit cell shrinks after Li extraction and expands after Li reinsertion, confirming a topotactic Li intercalation/deintercalation process (see Supporting Information, Figure S7 for in situ XRD results). The cell parameters extracted from XRD pattern fitting (see Supporting Information, Figure S6b) are listed in Table 1. The unit cell volume change is ~1.3% upon delithiation, in good agreement with the computationally predicted volume change of 1.1% for removal of one lithium per formula unit.

Figure 5d shows the voltage profile of $Li_{3-x}Na_xMnCO_3PO_4$ (sample composition is $Li_{2.67}Na_{0.63}Mn0.96CO_3PO_4$) for as-synthesized and ball-milled samples cycled at C/100 (2 mA/g) at room temperature. The discharge capacity of the as-synthesized sample is only ~50 mAh/g, but clearly shows two voltage "plateaus", centered at 3 and 4 V, respectively, consistent with computationally predicted voltages for the Mn^{2+}/Mn^{3+} and Mn^{3+}/Mn^{4+} redox couples (3.2 and 4.1 V, respectively). Ball milling with carbon improves the achievable capacity to ~135 mAh/g, which is larger than the theoretical one-electron capacity (115 mAh/g), and corresponds to ~1.2 Li insertion per formula. On the other hand the discharge curve becomes sloped, which may be due to much smaller particle size and a greater number of defects. XRD patterns of the charged samples (see Supporting Information, Figure S8) reveal similar peak shifts as in the Fe samples and confirm that the Li removal is topotactic. To investigate the redox activity of Mn, we collected X-ray absorption near edge structure (XANES) data for samples charged and discharged to different voltages (see Supporting Information, Figure S9). The edge position of XANES spectra (first inflection point on edge) is used for estimating the oxidation state of Mn compounds.[40] In our charged samples, the edge position clearly shifts to higher energy value, suggesting an increase of oxidation state. The opposite happens for the discharged samples. Using several Mn oxides as reference compounds, we attempted to obtain the oxidation state of Mn in our samples (see Supporting Information). The estimated Mn oxidation state of the fully charged sample (charged to 5 V) is +3.3. However, we would like to note that XANES features are known to be impacted by both oxidation state and local coordination environment (type of ligands, geometry, etc.). Hence, our analysis for the sidorenkite structure which has an uncommon environment where MnO_6 octahedra are connected with both PO_4 and CO_3 groups may not be as accurate as those for simple manganese oxides. On the basis of the XANES results, and the fact that the discharge capacity is larger than the one-electron capacity, it is likely that the Mn^{3+}/Mn^{4+}redox couple is, at least, partially active. But further work is required to reach conclusive evidence.

■ DISCUSSION

$Li_3FePO_4CO_3$ and $Li_3MnPO_4CO_3$ are two members of a novel mixed polyanion chemistry identified by a new approach to cathode discovery: high-throughput computational screening. The $Li_3FeCO_3PO_4$ compound shows a capacity very close to its theoretical one-electron value. The requirement for ball milling with carbon or higher cycling temperature indicates that kinetic factors may be limiting the material's performances. As DFT computations indicate that lithium diffusion can be fast enough in the isostructural $Li_3MnCO_3PO_4$, other possible limiting factors such as electronic conductivity,[41,42] surface effects[11] or antisite defects warrant further investigation. Overcoming such problems is typical for the development of Li-battery cathodes, as exemplified by $LiFePO_4$, which evolved from a low rate material[36] to a material with very high rate capability.[11] The good cycling performance of $Li_3FePO_4CO_3$, the small volume change, and the XRD of the charged compounds provide evidence that the crystal structure of the carbonophosphates is very suitable for the reversible intercalation of lithium.

For $Li_3MnPO_4CO_3$, both Mn^{2+}/Mn^{3+} and Mn^{3+}/Mn^{4+} redox couples are predicted to lie within the stability window of commercial electrolytes. Two-electron phosphate compounds operating in a 3 to 4.5 V voltage window are rare, especially when a 2+ to 4+ couple is sought.[43] Recent attempts to design such two-electron compounds in $Li_2FeP_2O_7$[44] and $Li_2MnP_2O_7$[44] did not succeed because of the high voltage of the Mn^{3+}/Mn^{4+} and Fe^{3+}/Fe^{4+} couples in a phosphate. While the theoretical capacity of $Li_3MnPO_4CO_3$ for a two-electron process is 231 mAh/g and its theoretical energy density is 859 W h/kg (a 45% improvement over $LiFePO_4$), so far only ~135 mAh/g was obtained experimentally. The poor electrochemical performance observed for the manganese carbonophosphate compared to the iron version could be due to many factors. The contrast between the rather poor measured rate performance of the Mn compound and the computed Li migration

dx.doi.org/10.1021/cm203243x | Chem. Mater. 2012, 24, 2009–2016

barrier seems to indicate that processes besides Li-ion conductivity are responsible for the limitations in capacity. For example, if electronic conductivity is limiting, carbon coating or other surface modifications may be needed to improve the transport through the electrode. In addition, the computed lithium mobility barriers have been obtained on a pure $Li_3MnPO_4CO_3$, but the significant amount of residual Na on the Li site after ion-exchange is likely to affect the capacity. As an example, the cycling curve of $Li_{2.27}Na_{0.81}FePO_4CO_3$ is shown in Supporting Information, Figure S10, and gives a reversible capacity of only ~15 mAh/g, much lower than that of the fully ion-exchanged $Li_3FeCO_3PO_4$ (Figure 5a). The most ion-exchanged sample of $Li_{3-x}Na_xMnCO_3PO_4$ obtained so far still contains ~19% Na on the Li site, and improving the ion-exchange rate of the Mn compound may be crucial to realize its high theoretical cycling capacity.

The Fe and Mn compounds demonstrate good reversibility of Li intercalation and deintercalation. Given that carbonophosphates have never been studied as intercalation cathodes, and that carbonophosphates are also generally a rarely studied chemical class in other fields, our knowledge on these compounds is still limited. Future studies of the intercalation mechanism and phase transitions during cycling may reveal the structural factors critical to improve the electrochemical performance.

CONCLUSIONS

High-throughput computational screening of materials is a new method for rapid and unbiased screening of novel chemistries given only minimum information on feasible synthetic routes (in our case the possibility of Na−Li exchange). We presented an example of such a search in the field of lithium ion batteries. Carbonophosphates, never synthesized before, were identified computationally, synthesized, characterized, and electrochemically tested. In particular, the Mn carbonophosphate $Li_3MnPO_4CO_3$ could potentially display a specific energy 45% greater than $LiFePO_4$ at low cost. While further optimization of these materials is still needed, the first electrochemical results are encouraging and demonstrate the promise for further optimization of this new class of chemistries and crystal structures.

ASSOCIATED CONTENT

Supporting Information

Further details are given in Figure S1−S10 and Tables S1−S5 together with a discussion of these results. This material is available free of charge via the Internet at http://pubs.acs.org.

AUTHOR INFORMATION

Corresponding Author

*E-mail: gceder@mit.edu.

Notes

The authors declare no competing financial interest.

ACKNOWLEDGMENTS

The authors acknowledge the Robert Bosch Company and Umicore for funding. A.J. acknowledges funding from the U.S. Department of Energy Computational Science Graduate Fellowship (DOE CSGF) under Grant DE-FG02-97ER25308. Y.T. acknowledges funding support from C.M. Hansel (Harvard University) though National Science Foundation. The authors also thank U.S. Department of Energy BATT program under Contract No. DE-AC02-05CH11231 for funding support. This research was supported in part by the National Science Foundation through TeraGrid resources provided by Texas Advanced Computing Center (TACC) under Grant TG-DMR970008S. The authors thank Dr. Clare Grey, Dr. Olivera Zivkovic, and Dr. Lin-shu Du for helpful discussions. The authors also thank the General User Program of the National Synchrotron Light Source for awarding synchrotron beam time and Dr. Peter Stephens and Dr. Jianming Bai for help with synchrotron XRD data collection. The structure prediction methods were funded by the Department of Energy, Basic Energy Sciences, under contract number DE-FG02-96ER45571. Work at Brookhaven National Laboratory, including the use of Center for Functional Nanomaterials, was supported by the U.S. Department of Energy, Office of Basic Energy Science, under Contract No. DE-AC02-98CH10886.

REFERENCES

(1) Whittingham, M. S. *Chem. Rev.* **2004**, *104*, 4271−4302.
(2) Ellis, B. L.; Lee, K. T.; Nazar, L. F. *Chem. Mater.* **2010**, *22*, 691−714.
(3) DiSalvo, F. J. *Pure Appl. Chem.* **2000**, *72*, 1799−1807.
(4) Jain, A.; et al. *Comput. Mater. Sci.* **2011**, *50* (8), 2295−2310.
(5) Armstrong, A. R.; et al. *Chem. Mater.* **2010**, *2*, 6426−6432.
(6) Arroyo-deDompablo, M. E.; et al. *Chem. Mater.* **2008**, *20*, 5574−5584.
(7) Frayret, C.; et al. *Phys. Chem. Chem. Phys.* **2010**, *12* (47), 15512−15522.
(8) Ong, S. P.; Jain, A.; Hautier, G.; Kang, B.; Ceder, G. *Electrochem. Commun.* **2010**, *4*, 1−4.
(9) Yamada, A. et al., *Adv. Mater. 8501* (**2010**).
(10) Kang, K.; Meng, Y. S.; Bréger, J.; Grey, C. P.; Ceder, G. *Science* **2006**, *311*, 977−980.
(11) Kang, B.; Ceder, G. *Nature* **2009**, *458*, 190−193.
(12) Hautier, G.; Fischer, C.; Ehrlacher, V.; Jain, A.; Ceder, G. *Inorg. Chem.* **2010**, *50*, 656−663.
(13) Hautier, G.; Fischer, C. C.; Jain, A.; Mueller, T.; Ceder, G. *Chem. Mater.* **2010**, *22*, 3762−3767.
(14) *ICSD Inorganic Crystal Structure Database*; Fachinformationszentrum Karlsruhe: Karlsruhe, Germany, 2006.
(15) Meng, Y. S.; Arroyo-de Dompablo, M. E. *Energy Environ. Sci.* **2009**, *2*, 589.
(16) Hautier, G.; et al. *J. Mater. Chem.* **2011**, *21* (43), 17147−17153.
(17) Kresse, G.; Furthmuller, J. *Comput. Mater. Sci.* **1996**, *6*, 15−50.
(18) Blöchl, P. *Phys. Rev. B* **1994**, *50*, 17953−17979.
(19) Perdew, J.; Burke, K.; Ernzerhof, M. *Phys. Rev. Lett.* **1996**, *77*, 3865−3868.
(20) Anisimov, V. I.; Aryasetiawan, F.; Lichtenstein, A. I. *J. Phys.: Condens. Matter* **1997**, *9*, 767−808.
(21) Monkhorst, H. J.; Pack, J. D. *Phys. Rev. B* **1976**, *13*, 5188−5192.
(22) H. Jónsson, G. M.; Jacobsen, K. W. In *Classical and Quantum Dynamics in Condensed Phase Simulations*; Berne, B. J., Ciccotti, G., Coker, D. F., Eds.; World Scientific Publishing Co. : Singapore, **1998**; p 385.
(23) Mills, G.; Jonsson, H. *Phys. Rev. Lett.* **1994**, *72* (7), 1124−1127.
(24) Armstrong, A. R.; Bruce, P. G. *Nature* **1996**, *381* (6582), 499−500.
(25) Toby, B. H. *J. Appl. Crystallogr.* **2001**, *34*, 210−213.
(26) Aydinol, M.; Kohan, A.; Ceder, G.; Cho, K.; Joannopoulos, J. *Phys. Rev. B* **1997**, *56*, 1354−1365.
(27) Kim, J. C.; et al. *J. Electrochem. Soc.* **2011**, *158* (3), A309−A315.
(28) Morgan, D.; Van der Ven, A.; Ceder, G. *Electrochem. Solid State Lett.* **2004**, *7* (2), A30−A32.
(29) Delmas, C.; Braconnier, J. J.; Hagenmuller, P. *Mater. Res. Bull.* **1982**, *17*, 117−123.

(30) Gaubicher, J.; Wurm, C.; Goward, G.; Masquelier, C.; Nazar, L. *Chem. Mater.* **2000**, *12*, 3240−3242.
(31) Hautier, G.; et al. *J. Mater. Chem.* **2011**, *21*, 17147−17153.
(32) Khomyakov, A. *Int. Geol. Rev.* **1980**, *22*, 811−814.
(33) Kurova, T. A.; Shumiatskaia, N. G.; Voronkov, A. A.; Piatenko, I. A. *Doklady Akademii Nauk Sssr* **1980**, *251* (3), 605−607.
(34) Kurova, T. A.; Shumyatskaya, N. G.; Vornkov, A. A.; Pyatenko, Y. A. *Mineralogiceskij Zhurnal* **1980**, *2*, 65−70.
(35) Khomyakov, A.; Aleksandrov, N. I.; Krasnova, V. V.; Ermilov, N. N.; Smol'yaninova. *Zap. Vses. Mineral. Obshch.* **1982**, *111*, 486−490.
(36) Padhi, A.; Nanjundaswamy, K.; Goodenough, J. B. *J. Electrochem. Soc.* **1997**, *144*, 1188.
(37) Oh, S. M.; et al. *Adv. Funct. Mater.* **2010**, *20* (19), 3260−3265.
(38) Bhattacharya, J.; Van der Ven, A. *Phys. Rev. B* **2010**, *81*, 104304.
(39) Kang, K.; Morgan, D.; Ceder, G. *Phys. Rev. B* **2009**, *79*, 1−4.
(40) Ressler, T.; Wong, J.; Roos, J. *J. Synchrotron Radiat.* **1999**, *6*, 656−658.
(41) Maxisch, T.; Zhou, F.; Ceder, G. *Phys. Rev. B* **2006**, *73*, 1−6.
(42) Ong, S.; Chevrier, V.; Ceder, G. *Phys. Rev. B* **2011**, *83*, 1−7.
(43) Hautier, G.; et al. *Chem. Mater.* **2011**, *23* (15), 3495−3508.
(44) Zhou, H.; et al. *Chem. Mater.* **2011**, *23* (2), 293−300.